Preparation and properties of polyaniline–anionic spherical polyelectrolyte brushes nanocomposite

Na Su[1], *Ping Gu*[1], *Junjie Zhao*[2]

[1]*School of Printing and Packaging Engineering, Shanghai Publishing and Printing College, Shanghai 200093, People's Republic of China*
[2]*School of Printing and Packaging, Wuhan University, Wuhan 430079, People's Republic of China*
E-mail: suna@whu.edu.cn

Published in Micro & Nano Letters; Received on 3rd August 2014; Revised on 6th November 2014; Accepted on 2nd January 2015

A novel polyaniline–anionic spherical polyelectrolyte brushes (PANI/ASPB) nanocomposite was synthesised by means of chemical oxidative polymerisation. Different characterisation and analytical methods involving scanning electron microscopy, Fourier transform infrared spectroscopy, X-ray diffraction and thermo-gravimetric analysis confirmed that anionic spherical polyelectrolyte brushes served both as a dopant and as a template. While polyaniline (PANI) nanocomposites have a 'rod-like' or fibrillar morphology, the PANI/ASPB nanocomposite displayed a sphere-like structure. The room temperature electrical conductivity of the PANI/ASPB nanocomposite was 26.3 S/cm, which is higher than that of PANI (7.1 S/cm). In addition, PANI/ASPB nanocomposites possessed enhanced thermal stability and good solubility properties.

1. Introduction: With the development of radio-frequency identification (RFID) technology, the applications of printed electronics have attracted great interest [1–3] recently. The RFID tag is a typical example of a comprehensive application of electronic technology and substrates, to achieve communication between the substrates and the computer. The printing method of RFID tags by conductive ink is environmentally friendly, efficient and of low cost [4]. Therefore, the excellent properties of conductive ink and efficient printing are the focus of our research. On one hand, among the extensive studies of conducting polymers, polyaniline (PANI) is of particular interest because of its ready availability, easy synthesis, excellent physical and chemical properties, and good environmental stability [5, 6]. However, pristine PANI is insoluble and infusible because of the rigidity of its molecular chains of a π-conjugated structure, leading to limited application on a large scale [7]. To overcome these shortcomings, the synthesis of PANI with suitably modified structures by both electrochemical [8, 9] and chemical routes [10–12] has been performed. On the other hand, as the fastest growing printing technology in recent years, inkjet printing is one of the easiest technologies to achieve miniaturisation. The digital information in the computer can be directly sprayed onto materials of any shape. The production of RFID tags includes inkjet printing and gilding, avoiding the materials being cut and saving costs. At the same time, the printing ink of RFID tags needs to have good liquidity to prevent the nozzle from clogging [13]. In view of this, anionic spherical polyelectrolyte brushes (ASPBs) may be a template for and a novel dopant of conducting polymers, not only because of their spherical structure, which can provide the growth of spherical morphology for conducting polymers, but also because of their charged chains. The thermal stability, electrical conductivity and the solubility of the composites are enhanced by controlling the thickness of brush layers and/or the proportion of ASPBs in the composites.

In this Letter, we present a facile method for the synthesis of PANI/ASPB nanocomposite by chemical oxidative polymerisation. For comparison, PANI and ASPBs were synthesised ahead. An ASPB is poly(sodium-p-styrenesulfonate) (PSS)-coated SiO_2 [14]. The morphology of the resulting PANI/ASPB nanocomposite was studied by scanning electron microscopy (SEM). Information about its bonding structure was obtained from Fourier transform infrared spectroscopy (FTIR) and X-ray diffraction (XRD) techniques were useful in understanding its crystallographic structure. The room temperature electrical conductivity, thermal stability and solubility of PANI and PANI/ASPB nanocomposites were investigated by a four-point probe apparatus, thermo-gravimetric analysis (TGA) and a DDS-12A Digital Conductivity Meter, respectively.

2. Experimental: The preparation method of ASPBs is described elsewhere [14]. In a typical procedure, 51 mg of ASPBs was first added into 21 ml of 2 M HCl (aq), and then the mixture was dispersed by an ultrasonic dispersion machine for 20 min. After adding 1.0 ml of aniline, the mixture was cooled to 5°C and degassed under a flow of nitrogen for 20 min followed by the addition of 2.5 g of ammonium persulphate. The reaction was maintained for 6 h. The products were then collected via filtration, and washed three times using ethanol and distilled H_2O before finally being vacuum dried at 60°C for 24 h.

The chemical composition of PANI/ASPB nanocomposites was investigated by an energy dispersive X-ray diffraction (EDX) spectrometer attached to a Quanta 200 (FEI, The Netherlands) scanning electron microscope operated at 30 kV. FTIR spectroscopy was recorded on a Nicolet AVATAR 360FT spectrometer (USA). XRD patterns of samples were obtained using a piece of equipment (Shimadzu XRD-6000, Japan) operating at a voltage of 40 kV and a current of 40 mA with Cu K_α radiation, $\lambda = 1.54060$ Å. A continuous scan mode at 5–50° (2θ) with a scanning rate of 5°/min was conducted. TGA was carried out on a SETSYS-1750 instrument at a constant rise of temperature (10°C/min) under N_2 atmosphere.

The electrical conductivity was measured in a four-point probe (RTS-4, China) apparatus at room temperature. After being vacuum dried at 60°C for 24 h, the samples were compressed into a circular tablet with a diameter of 13 mm and a thickness greater than 1 mm at 20 MPa. The thickness W of each tablet was measured accurately using a Vernier Caliper. F (W/S) and F (D/S) ($S = 1$), which denote the width correction coefficient and the diameter correction coefficient, respectively, were taken from a reference to calculate the source current I according to the formula (1) [15]

$$I = F(W/S) \times F(D/S) \times W \times 0.1 \quad (1)$$

The room temperature resistivity ρ was then obtained from the four-point probe apparatus. Since conductivity (σ; S/cm) = $1/\rho$, the electrical conductivity of products could be calculated.

The solubility of the samples is reflected by the conductivity of the saturated solution ($T = 25$ °C and pH = 6), which was measured using a DDS-12A digital conductivity meter (Hubei Provincial Institute of Measurement and Testing). The process is as follows: 10 mg of samples was dissolved in 4 ml of ethanol, stirred and heated to boiling, followed by removal of the supernatant and soluble impurities. The method described above was repeated twice. To make the samples fully dissolved, 10 ml of ethanol was added and heated to boiling. The sample was placed in a constant temperature bath for 20 min to precipitate the solid and 3 or 4 ml of supernatant was then taken into the beaker for fear of affecting the test result because of the solid particles suspended in the electrode. The conductivity of the saturated solution of ethanol was required to determine references.

3. Results and discussion: For the purpose of obtaining a clear insight into the morphology of the resulting PANI/ASPB nannocomposite, a SEM test was carried out. Fig. 1 displays the morphologies of PANI (Fig. 1*a*), PANI/ASPB nanocomposite (Fig. 1*b*) and ASPBs (Fig. 1*c*). The chemical composition of the PANI/ASPB nanocomposite was determined by simultaneous EDX spectroscopy (Fig. 1*d*). As observed from Fig. 1*a*, PANI shows a typical 'rod-like' or a fibrillar structure [16]. The structure of PANI is stretched with a length of ca. 700 nm, diameter of (100 ± 10) nm and with a narrow diameter distribution. The micrograph of the PANI/ASPB nanocomposite (Fig. 1*b*) shows a spherical-like structure. This may be because the addition of ASPB with uniform spherical structure (Fig. 1*c*) provides the space factors for the orderly growth of PANI. ASPBs serve as a template for the synthesis of the PANI/ASPB nanocomposite. EDX analysis was used to investigate the chemical composition of the PANI/ASPB nanocomposite (Fig. 1*d*). The signal corresponding to silicon appears on the spectrum, indicating that the doping of ASPBs in a PANI matrix has indeed taken place.

Next, the chemical structure of samples was studied by FTIR spectroscopy (Fig. 2). The characteristic bands of protonated PANI, represented by the absorption bands at 1567 and 1489 cm^{-1}, are

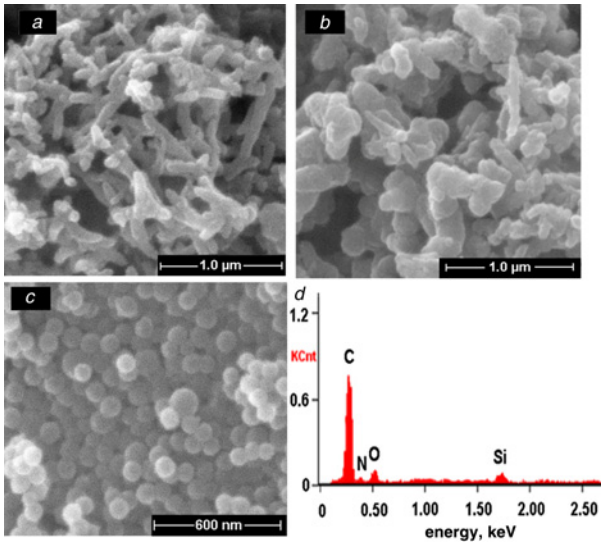

Figure 1 *SEM images*
a PANI
b PANI/ASPB nanocomposite
c ASPBs
d EDX analysis of PANI/ASPB nanocomposite

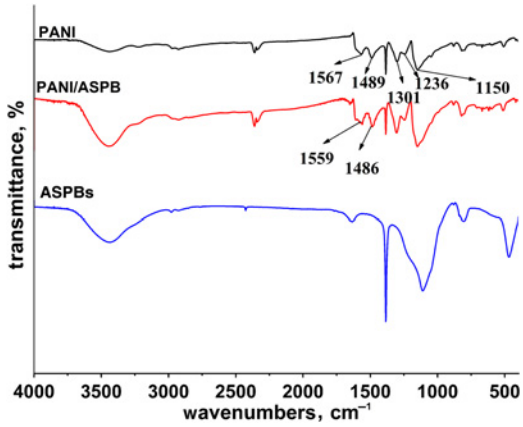

Figure 2 *FTIR spectra of PANI, PANI/ASPB nanocomposite and ASPBs*

assigned to the stretching vibration of the quinonoid and benzenoid rings. The appearance of peaks at 1301 and 1203 cm^{-1} can be attributed to C–N and C = N stretching vibrations, respectively, which is consistent with the literature [17]. When doped with ASPBs, no new peaks occur, which proves that the structure of PANI chains is not affected by the dopant ions. However, the positions of the two peaks have shifted to low frequency (1559 and 1486 cm^{-1}). The reason may be that chemical oxidative polymerisation doping enhances the delocalisation of charge electrons, and the bond force constant of carbon in the quinone ring is reduced [18]. The result further explains that the improvement of electrical conductivity of PANI/ASPB nanocomposite is because of the delocalisation effects of radical cations [19].

XRD experiments were performed to analyse the crystallographic structure of the samples. It can be observed from Fig. 3 that ASPBs only exhibit a broad characteristic peak at $2\theta = 24.4°$, corresponding to the SiO_2 reflection peak. For the XRD pattern of PANI, the characteristic peaks at $2\theta = 9°$, 15.4°, 20.2° and 25° are attributed to the structure of parallel polymer chains interlaced with vertical and periodically oriented polymer chains [20]. For the PANI/ASPB nanocomposite, since the ratio of [Cl]/[N] in the nanocomposite is reduced, the intensity of the peak at 21° is increased [21] and the location and intensity of the remaining peaks are changed. The peaks move to $2\theta = 8.5°$, 15°, 21° and 25.4°, respectively. When the diffraction peaks are $2\theta = 8.5°$, 15°, 21° and 25.4°, the interplanar distance (d) is 1.06, 0.58, 0.42 and 0.35 nm, separately calculated by the Prague formula ($2d \sin\theta = n\lambda$). The full width at half maximum (FWHM) of PANI at $2\theta = 25°$ is 2.4°, and the PANI/ASPB nanocomposite at $2\theta = 25.4°$ is 3°. The FWHM of the PANI/

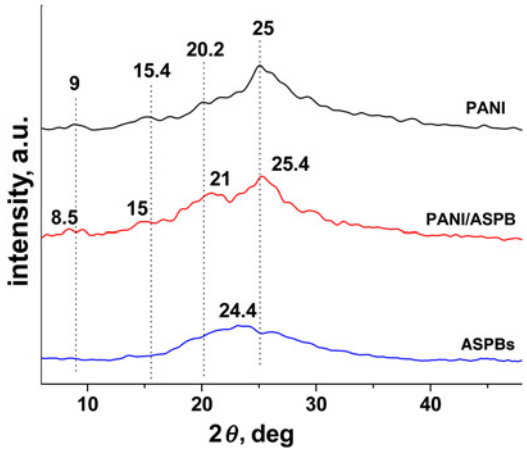

Figure 3 *XRD patterns of PANI, PANI/ASPB nanocomposite and ASPBs*

doi: 10.1049/mnl.2014.0451

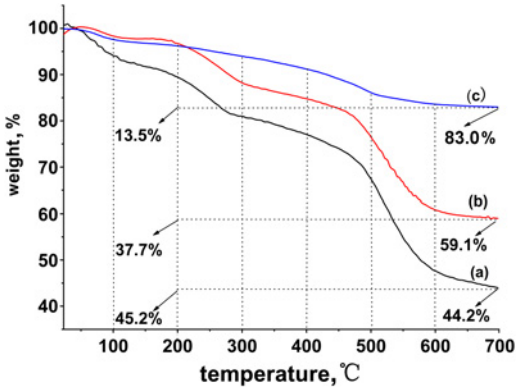

Figure 4 *TGA curves*
a PANI; *b* PANI/ASPB nanocomposites; *c* ASPBs

ASPB nanocomposite increases, demonstrating the nanocomposite with low crystallinity and small particle size. As a result, the solubility of the PANI/ASPB nanocomposite in ethanol improves.

The electrical conductivities of PANI and PANI/ASPB nanocomposite are determined using a RTS-4 four-point probe resistivity measurement system. The results suggest that the room-temperature electrical conductivity of PANI is 7.1 S/cm. However, the PANI/ASPB nanocomposite shows a high value of electrical conductivity (26.3 S/cm). The increase in magnitude of electrical conductivity may be due to the fact that the polyelectrolyte chains of ASPBs are favourable to the orderly growth of aniline monomers, leading to a higher conjugate length. This is consistent with the trends of the SEM and FTIR analysis results.

Fig. 4 displays the TGA of (a) PANI, (b) PANI/ASPB nanocomposite and (c) ASPBs under N_2 atmosphere at 60% RH. As observed from Fig. 4, curves *c* and *a*, the thermal stability of ASPBs is much higher than that of PANI in the temperature range of 35–700°C. As PANI is hygroscopic, nearly 5.9 wt% loss has occurred at 100°C, because of the evaporation of residual water, while there is only 1.7 wt% weight loss for PANI/ASPB nanocomposite (see Fig. 4, curve *b*). As the temperature increases, the main mass loss of PANI and PANI/ASPB nanocomposite starts at about 200°C, corresponding to the PANI degradation [22]. As shown in Fig. 4, curves *a* and *b*, the weight loss for PANI is 45.2%, more than that for the PANI/ASPB nanocomposite (37.7%). The enhancement in thermal stability has been seen for PPy/ASPB nanocomposite, which is of significance for the preparation of high-performance conductive composites.

Fig. 5 represents the solubility of the samples, which is reflected by the conductivity of the saturated solution ($T = 25$°C and pH = 6). As shown in Fig. 5*a*, different amounts of ASPBs in the PANI/ASPB nanocomposite (10 mg) were dissolved in ethanol (4 ml)

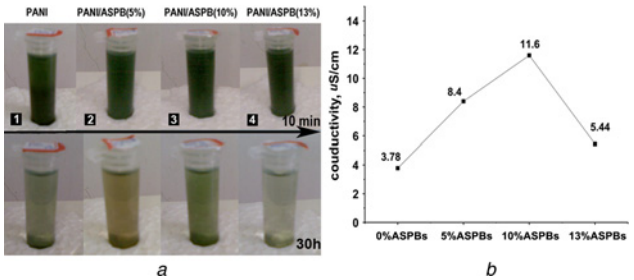

Figure 5 *Pictures of the conductivity of saturated solution of PANI/ASPB nanocomposite with different amounts of ASPBs ($T = 25$°C and pH = 6), and results of quantitative analysis method*
a Conductivity of saturated solution of PANI/ASPB nanocomposite with different amounts of ASPBs
b Results of quantitative analysis method

with ultrasonic dispersion for 10 min, and left for 30 h. If the conductive composite has good solubility, its solution should be green. When 5 wt% of ASPBs is added, the solution shows green, indicating good solubility of the nanocomposite, which is consistent with the results of the XRD. The main reason is that the resulting PANI chains become short and small because of the PSS flexible long chains, which makes the nanocomposite well dissolved in the solvent. Further, the solubility of the PANI/ASPB nanocomposite is also changed by adding different amounts of ASPBs. When 10 wt% of ASPBs is added, a dark green colour of the solution is obtained. When the amount of ASPBs is increased to 13 wt%, the solution becomes clear, indicating that excessive ASPBs will make the solubility of nanocomposite to decrease. The quantitative analysis method is also shown in Fig. 5*b*. The conductivity of the saturated solution of ethanol is 0.2 µS/cm. When ASPBs are added in amounts of 5, 10 and 13 wt%, the solution conductivities are 8.4, 11.6 and 5.44 µS/cm, respectively. The increase in the amount of ASPBs in the PANI/ASPB nanocomposite will enhance the solubility of PANI, but excessive ASPBs will decrease the solubility of PANI because of the effect of the SiO_2 cores [23].

Fig. 6 represents the mechanism of the reaction process. The polymerisation reaction of aniline monomers occurs in the PSS chains in the presence of ASPBs. We can see that the amount of positive charge per unit length in PANI chains is much less than the amount of negative charge per unit length in PSS chains. Therefore, part of SO_3^- is balanced by Na^+. The addition of aniline monomer increases its effective concentration in PSS chains by exchange of Na^+. Since the influences of the density gradient formed by densely grafted PSS chains, polymerisation reaction take place preferentially in high-concentration aniline monomers which are situated in the cores of the ASPBs. According to the doping mechanism of protonic acid, reaction occurs first at the imine nitrogen atom of polymer chains, producing the protonated imine nitrogen atom to form a polymeric cationic. Thus, polycations play the role of multivalent counterions in brush layers and strong complexation between PSS and PANI occurs. Therefore, the polymerisation reaction of aniline monomers is fixed in the brush layers. To sum up, ASPBs serve as a template

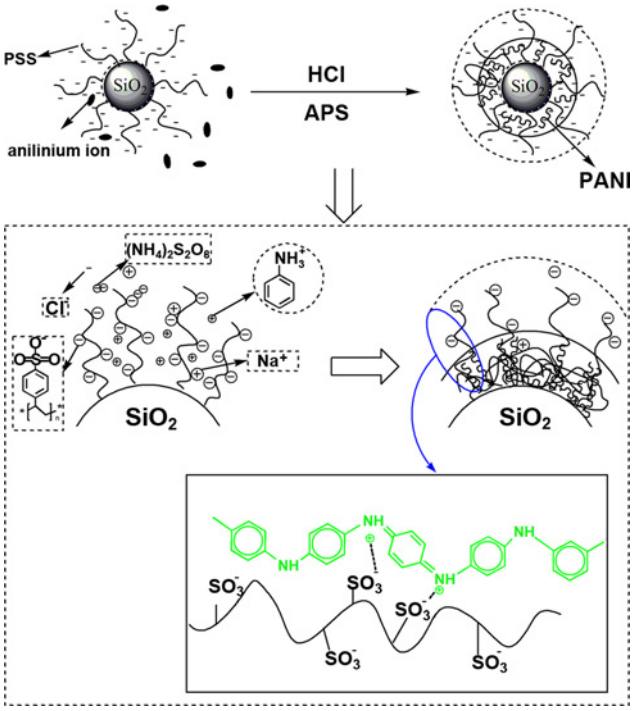

Figure 6 *Schematic representations of the mechanism of the reaction process*

for the synthesis of PANI/ASPB nanocomposite by capturing and controlling the type and number of ions in brush layers in the manner of electrostatic interaction [24].

4. Conclusion: In summary, a novel PANI/ASPB nanocomposite by means of the chemical oxidation polymerisation method has been described. Different characterisation and analytical methods confirm that ASPBs serve both as a dopant and as a template. Compared with PANI, PANI/ASPB nanocomposite possesses the appearance of a sphere-like structure, enhanced room temperature electrical conductivity, improved thermal stability and good solubility. The resulting PANI/ASPB nanocomposite is expected to be applied in RFID tags and inkjet printing.

5. Acknowledgments: This research was supported by the Scientific Research Foundation for the Introduction of Talents of the Shanghai Publishing and Printing College (2014BSKY06).

6 References

[1] Cho J., Shin K.H., Jang J.: 'Micropatterning of conducting polymer tracks on plasma treated flexible substrate using vapor phase polymerization-mediated inkjet printing', *Synth. Met.*, 2010, **160**, pp. 1119–1125

[2] Hara K., Kurashige M., Ito S., Shinpo A., Suga S., Sayama K., Arakawa H.: 'Novel polyene dyes for highly efficient dye-sensitized solar cells', *Chem. Commun.*, 2003, pp. 252–253

[3] Li X.F., Hao X.F., Yu H.B., Na H.: 'Fabrication of polyacrylonitrile/polypyrrole (PAN/Ppy) composite nanofibres and nanospheres with core–shell structures by electrospinning', *Mater. Lett.*, 2008, **62**, pp. 1155–1158

[4] Shirakawa H., Louis E.J., MacDiarmid A.G., Chiang C.K., Heeger A.J.: 'Synthesis of electrically conducting organic polymers: halogen derivatives of polyacetylene, $(CH)_x$', *J. Chem. Soc. Chem. Commun.*, 1977, **1977**, pp. 578–580

[5] Vhanakhande B.B., Jadhav S.V., Kulkarni D.C.: 'Investigation on the microwave properties of electropolymerised polyaniline thin film', *Microw. Opt. Technol. Lett.*, 2008, **50**, pp. 761–766

[6] Lin Q.Q., Li Y., Yang M.J.: 'Polyaniline nanofiber humidity sensor prepared by electrospinning', *Sens. Actuators B, Chem.*, 2012, **161**, pp. 967–972

[7] Hatchett D.W., Josowicz M.: 'Composites of intrinsically conducting polymers as sensing nanomaterials', *Chem. Rev.*, 2008, **108**, pp. 746–769

[8] Diaz A.F., Logan J.A.: 'Electroactive polyaniline films', *J. Electroanal. Chem.*, 1980, **111**, pp. 111

[9] Chowdhury A.N., Rahman M.R., Islam D.S.: 'Electrochemical preparation and characterization of conducting copolymer/silica composite', *J. Appl. Polym. Sci.*, 2008, **110**, pp. 808–816

[10] Denga H., Caoa Q., Wanga X.: 'Studies on preparation and properties of the multi-walled carbon nanotubes (MWNTs)/epoxy nanocomposites', *Mat. Sci. Eng. A*, 2011, **528**, pp. 5759–5763

[11] Porramezan M., Eisazadeh H.: 'Fabrication and characterization of polyaniline nanocomposite modified with Ag_2O', *Nanoparticles Compos. B*, 2011, **42**, pp. 1980–1986

[12] Wanga Y., Shia Y., Xua X.: 'Preparation of PANI-coated poly (styrene-co-styrene sulfonate) nanoparticles in microemulsion media', *Colloids Surf. A, Physicochem. Eng. Aspects*, 2009, **345**, pp. 71–74

[13] Hubbe M.A., Heitmann J.A., Cole C.A.: 'Water release from fractionated stock suspensions – Part 2: Effects of consistency, flocculants, shear, and order of mixing', *Tappi J.*, 2008, **7**, pp. 14–19

[14] Su N., Li H.B., Zheng H.M., Yi S.P., Liu X.H.: 'Synthesis and characterization of poly(sodium-p-styrenesulfonate)/modified SiO_2 spherical brushes', *eXPRESS Polym. Lett.*, 2012, **6**, pp. 680

[15] Su N., Li H.B., Yuan S.J., Yi S.P., Yin E.Q.: 'Synthesis and characterization of polypyrrole doped with anionic spherical polyelectrolyte brushes', *eXPRESS Polym. Lett.*, 2012, **6**, pp. 697–705

[16] Mavundla S.E., Malgas G.F., Motaung D.E., Iwuoha E.I.: 'Physicochemical and morphological properties of poly (aniline-co-pyrrole)', *J. Materi. Sci.*, 2010, **45**, pp. 3325–3330

[17] Kulkarni M.V., Viswanath A.K., Marimuthu R., Seth T.: 'Spectroscopic, transport, and morphological studies of polyaniline doped with inorganic acids', *Polym. Eng. Sci.*, 2004, **44**, pp. 1676–1681

[18] Kofranek M., Kovar T., Karpfen A.: 'Abinitio studies on heterocyclic conjugated polymers: structure and vibrational spectra of pyrrole, oligopyrroles and polypyrrorle', *J. Chem. Phys.*, 1992, **96**, pp. 4464

[19] Munstedt H.: 'Properties of polypyrrole treated with base and acid', *Polymer*, 1986, **27**, pp. 899

[20] Wang J.S., Wang J.X., Yang Z.: 'A novel strategy for the synthesis of polyaniline nanostructures with controlled morphology', *React. Funct. Polym.*, 2008, **68**, pp. 1435–1440

[21] Pouget J.P.: 'X-ray structure of polyaniline', *Macromolecules*, 1991, **24**, pp. 779–789

[22] Kang S., Hong S., Choe C.R.: 'Preparation and characterization of epoxy composites filled with functionalized nanosilica particles obtained via sol–gel process', *Polymer*, 2001, **42**, pp. 879–887

[23] Yin W., Ruckenstein E.: 'Soluble polyaniline co-doped with dodecyl benzene sulfonic acid and hydrochloric acid', *Synth. Met.*, 2000, **108**, pp. 39–46

[24] Korovin A.N., Sergeyev V.G., Pyshkina O.A.: 'Nanoreactor-assisted polymerization toward stable dispersions of conductive composite particles', *Macromol. Rapid Comm.*, 2011, **32**, pp. 462–467

doi: 10.1049/mnl.2014.0451